Constraints on MARID petrogenesis: SHRIMP II U-Pb zircon evidence for pre-eruption metasomatism at Kampfersdam

Hamilton, M.A.[1], Pearson, D.G.[2], Stern, R.A.[1], and Boyd, F.R.[3]

1. J. C. Roddick Ion Microprobe Laboratory, Geological Survey of Canada, 601 Booth St., Ottawa, Ontario, K1A 0E8 Canada
2. Department of Geological Sciences, University of Durham, South Road, Durham, DH1 3LE U.K.
3. Geophysical Laboratory, Carnegie Institution of Washington, 5251 Broad Branch Road, N.W., Washington, D.C. 20015 U.S.A.

It has become increasingly evident in recent years that zircon xenocrysts recovered from kimberlite can comprise complex populations whose U-Pb ages may document either zircon crystallisation from the protokimberlite magma, or melt interaction with the sub-continental mantle at some earlier time. Only in rare cases has it been possible to precisely constrain mantle metasomatic ages (e.g. Kinny and Dawson, 1992); for the most part these ages, and their relationship to kimberlite magmas sampled in the overlying crust, are poorly known. In other instances, lithospheric enrichment by fluid or melt migration episodes, chronicled through U-Pb dating of monazite- and zircon-bearing glimmerite xenoliths in alkalic Eocene minette of the Wyoming craton (Rudnick et al., 1993; Carlson and Irving, 1994), has been indirectly linked to tectonomagmatic events documented at the surface in bounding orogens.

In order to further assess the timing of metasomatism within mantle peridotite, we have initiated a study of a MARID xenolith from the Kampfersdam kimberlite. Based on U-Pb ages of loose zircon megacrysts from the kimberlite matrix, Davis (1977) determined a late Cretaceous age (86.9 ± 1.1 Ma) for intrusion of the Kampfersdam pipe. The age is typical of numerous other (80-95 Ma) Group I kimberlites emplaced into Kaapvaal craton, particularly in the Kimberley region.

The MARID nodule, FRB 836, is approximately 15 cm in diameter, comprising a phlogopite-rich host together with a well-delimited vein of pale green amphibole 0.5 cm wide as well as irregular blebs and segregations of amphibole. Individual amphibole grains reach 4 mm in size. No flow textures are associated with the vein. Grains of amphibole are also dispersed throughout the micaceous matrix. The mica in FRB 836 is darker and more reddish-brown than that in glimmerites, has a grain size of 0.5-1 mm, and is not deformed. Apatite is dispersed throughout the mica host and vein, whereas irregular blebs of polygranular ilmenite are confined to the mica host only. Rare zircon is locally present, dispersed within phlogopite-rich zones or between phlogopite and amphibole grains or aggregates.

In an analysed thick section of FRB 836, a single, slightly elongate, xenomorphic zircon grain approximately 500x800 μm in size was selected for trace element and U-Pb analysis. Cathodoluminesce (CL) imaging reveals a weak but sharp concentric zoning at 50-70 μm widths, slightly offset from the grain center at one end of the crystal. Although several irregular fractures are present, the zircon is free of inclusions or rims, and lacks any overgrowths of baddeleyite.

Full rare earth element (REE) analysis and a suite of minor and trace element abundances were determined on the single zircon grain using a Cameca 4f ion probe at the University of Edinburgh. Shown in Figure 1 are chondrite-normalised REE abundances for two analyses of core domains (broadly dark in CL imagery), and two spot analyses in rim regions (broadly correlating with a lighter CL zone). As with many crustal zircons, both core and rim patterns show positive Ce anomalies, and weak negative Eu anomalies. Analyses from the grain centre have distinctly higher levels of total REE, rising steadily from La (~0.4 ppm) through Sm, with the patterns flattening out from Gd to Lu (~9 ppm). Rim compositions have an order-of-magnitude lower concentration, but with patterns mimicking those in the core, ranging from ~0.04 ppm La through to ~1.4 ppm Lu. Subtle differences nonetheless exist: core compositions are characterised by flatter HREE profiles (Lu/Sm ~ 1.2) and smaller Ce anomalies (Ce/Ce* ~ 4.2) than in the rim (Lu/Sm ~ 6.5; Ce/Ce* ~ 20). Elevated abundances of the REE correlate directly with Y(220-300 ppm) and Nb (7-11 ppm) concentrations, in contrast to distinctly lower values near the grain edge (~ 40 ppm Y, ~ 0.5 ppm Nb). Electron microprobe analyses Hf concentrations range from 1.04 (rim) to 1.35 (core) wt% HfO_2, and Zr/Hf ratios fall between 41.7 and 55.1, respectively, though six of eight spot analyses have an average Zr/Hf of 44.7 ± 1.2, regardless of position. These abundances and Zr/Hf ratios are within the compositional spectrum of most kimberlitic zircons, but do not show the stronger

depletion in Hf and higher Zr/Hf observed in megacrysts from Mbuji Mayi and from Jwaneng (Zr/Hf up to 114; Schärer et al., 1997; Kinny et al., 1989).

The strong chemical zonation illustrated within this zircon is suggestive of crystallisation under radically changing fluid/melt compositions; preservation of these variations is testimony to the sluggishness of these cations (including U, Th; see below) to diffuse even under upper mantle conditions.

FRB 836 zircon was dated *in situ* using the SHRIMP II ion microprobe at the Geological Survey of Canada in Ottawa, following initial CL and backscatter imaging at the GSC and trace element characterization using the University of Edinburgh ion probe. Prior to U-Pb analysis, the thick section was implanted with several grains the GSC's ion probe zircon standard (Stern, 1997; Kipawa, 993 Ma, ~250 ppm U). A total of 22 spots, each having a diameter of roughly 25x30 µm, were analysed in transverse sections across the grain and orthogonal to CL zonation. Data were accumulated in routines consisting of seven scans within any given pit. Reproducibility of the $^{206}Pb/^{238}U$ ratio in the standard was ±1.5% (1s), and propagated to the unknown spots.

Uranium and thorium abundances within the MARID zircon show considerable range, from 8-107 ppm and 3-104 ppm, respectively. Rim compositions have consistently low U (<30 ppm) and Th (<20 ppm) concentrations, and generally overlap with those characteristic of kimberlitic zircons (megacrysts) as illustrated in Figure 2. There is a steady and smooth increase in Th/U ratio from ~0.29 along the grain rim to ~0.97 in core regions, where U and Th concentrations reach a maximum of approximately 100 ppm. Although U concentrations in this grain are comparable to those found in the younger Jwaneng kimberlitic zircons (maximum 71 ppm; Kinny et al, 1989), they are in all cases distinctly higher in Th content and Th/U than the latter (<0.22). Compared to other mantle-derived zircons, the sample is intermediate in composition and Th/U between typical low-U and -Th kimberlitic zircon megacrysts and zircon included in diamond from Mbuji Mayi (Zaire; Kinny and Meyer, 1994). However, the most enriched Th and U compositions from FRB 836 zircon are similar to rare zircon compositions reported from certain Canadian carbonatites by Heaman et al. (1990). Conversely, MARID suite vein zircons from xenoliths in Bultfontein kimberlite (Kinny and Dawson, 1992), have considerably higher Th, U, and Th/U (Fig. 2), are distinct from the zircon compositions described here, and have presumably precipitated from significantly more evolved melts.

Uncorrected U-Pb isotopic data for FRB 836 zircon are presented on a Tera-Wasserburg plot in Figure 3. Measured radiogenic Pb (Pb*) concentrations are consistently low (≤3 ppm), and minor corrections for common Pb were necessary (non-radiogenic proportions of total ^{206}Pb range from 0.1 - 5.3%). Most spot analyses, however, are tightly clustered within a narrow range of $^{238}U/^{206}Pb$ ratios near concordia and yield a weighted mean age of 120 ± 2 Ma (2σ; N=18). This age excludes four analyses which disperse to slightly higher $^{238}U/^{206}Pb$ ratios, interpreted to reflect Pb-loss, either recently, or during entrainment via kimberlite eruption. Non-exclusion of two of these (highest $^{238}U/^{206}Pb$ ratios in Figure 3) results in an immaterial change to the weighted mean age - 119 ± 2 Ma; therefore, 120 ± 2 Ma is regarded as the best estimate of the crystallisation age of zircon in the metasomite FRB 836.

A striking feature of Fig. 3 is that little to none of the U-Pb data show evidence of resetting towards the age of the younger host kimberlite. Indeed, there is a complete lack of any spatially correlated age variation within the grain. In contrast to the metasomatised Bultfontein peridotite studied by Kinny and Dawson (1992), at Kampfersdam we find a distinct age separation between the timing of MARID metasomatism (120 Ma) and the eruption of host kimberlite (ca. 87 Ma), and that these two specific igneous suites cannot be linked. Moreover, the 120 Ma metasomatic event is significantly older than most Group I kimberlites in the Kimberley region. Significantly, the timing of metasomatism is coincident with the earliest of the pulses of Cretaceous kimberlites - (Group II) or orangeites, which for the most part erupted within the span of at least 115-150 Ma (Smith et al., 1985). The results presented here represent the first documentation of a MARID-assemblage xenolith yielding a cystallisation age substantially and unambiguously older than its host kimberlite. FRB 836 records a transient earlier metasomatic event that affected the shallow subcontinental mantle beneath the Kaapvaal craton and which was scavenged some 33 Myr later. The correspondence in age of the MARID zircon to the main phase of Group II kimberlite eruption through the Kaapvaal craton offers strong support for genetic models, based on phase equilibria results (Sweeney et al., 1993) for the MARID association involving derivation from Group II kimberlite magmas.

References
Carlson, R.W., and Irving, A.J., 1994, Depletion and enrichment history of subcontinental lithospheric mantle: An Os, Sr, Nd and Pb isotopic study of ultramafic xenoliths from the northwestern Wyoming Craton: Earth Planet. Sci. Letters, v.126, p. 457-472.
Davis, G.L., 1977, The ages and uranium contents of zircons from kimberlites and associated rocks: Carnegie Inst. Washington Yearbook, v. 76, p. 631-635.
Heaman, L.M., Bowins, R., and Crocket, J., 1990, The chemical composition of igneous zircon suites: implications for geochemical tracer studies: Geochim. et Cosmochim. Acta, v.54, p.1597-1607.
Kinny P.D., and Dawson, J.B., 1992, A mantle metasomatic injection eventlinked to late Cretaceous kimberlite magmatism: Nature, v. 360, p. 726-728.
Kinny P.D., and Meyer, H.O.A, 1994, Zircon from the mantle: A new way to date old diamonds: Jour. Geology, v. 102, p. 475-481.
Kinny, P.D., Compston, W., Bristow, J.W. and Williams, I.S., 1989, Archean mantle xenocrysts in a Permian kimberlite: Two generations of kimberlitic zircon in Jwaneng DK2, southern Botswana, *in* Kimberlites and Related Rocks: Geol. Soc. Australia Spec. Pub. 14, p. 833-842.
Rudnick, R.L., Irving, A.J., and Ireland, T.R., 1993, Evidence for 1.8 Ga mantle metasomatism beneath the northwestern margin of the Wyoming craton from SHRIMP analyses of zircons in ultramafic xenoliths: EOS, v. 74, p. 320.
Schärer, U., Corfu, F., and Demaiffe, D., 1997, U-Pb and Lu-Hf isotopes in baddeleyite and zircon megacrysts from the Mbuji-Mayi kimberlite: constraints on the subcontinental mantle: Chem. Geology, v. 143, p.1-16.
Smith, C.B., Gurney, J.J., Skinner, E.M.W., Clement, C.R., and Ebrahim, N., 1985, Geochemical character of southern African kimberlites: A new approach based on isotopic constraints: Trans. Geol. Soc. S. Afr., v. 88, p. 267-280.
Stern, R. A., 1997, The GSC Sensitive High Resolution Ion Microprobe (SHRIMP): analytical techniques of zircon U-Th-Pb age determinations and performance evaluation, *in* Radiogenic Age and Isotopic Studies, Report 10: Geol. Surv. Canada Current Research 1997-F, p. 1-31.
Sweeney, R.J., Thompson, A.B., and Ulmer, P., 1993, Phase relations of a natural MARID composition and implications for MARID genesis, lithospheric melting and mantle metasomatism: Contr. Mineralogy Petrology, v. 115, p. 225-241.

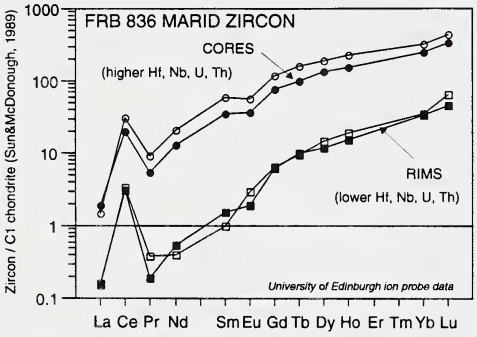

Figure 1. Chondrite-normalised rare earth element profiles for MARID suite zircon FRB 836.

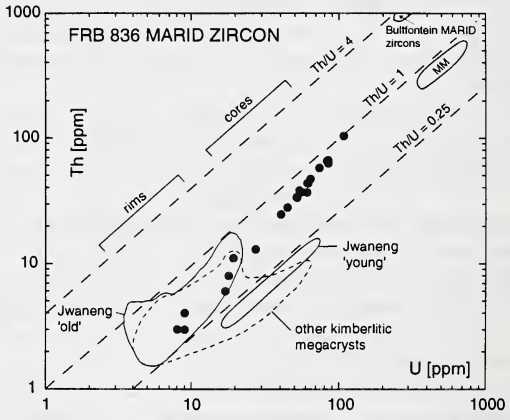

Figure 2. U and Th abundances in MARID zircons of this study, and of other mantle zircons. MM = diamond inclusion zircon from Mbuji Mayi. See text for data sources.

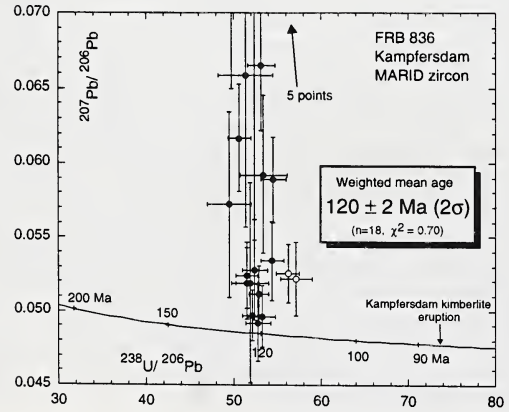

Figure 3. U-Pb (Tera-Wasserburg) concordia diagram showing uncorrected (for common Pb) SHRIMP II data for FRB 836 MARID zircon. Errors shown are 1σ. Pb/U ages are referred to Kipawa zircon at 993 Ma; Pb/U 1σ = 1.5%. Open symbols are spot analyses excluded from weighted mean. Mean age calculated from data using ^{207}Pb-method of common Pb correction.